International Journal of Heat and Mass Transfer 52 (2009) 5293–5301

Contents lists available at ScienceDirect

International Journal of Heat and Mass Transfer

journal homepage: www.elsevier.com/locate/ijhmt

Influences of nozzle-plate spacing on boiling heat transfer of confined planar dielectric liquid impinging jet

Chang Hwan Shin, Kyung Min Kim, Sung Hwan Lim, Hyung Hee Cho *

Department of Mechanical Engineering, Yonsei University, Seoul 120-749, Republic of Korea

ARTICLE INFO

Article history:
Received 13 January 2009
Received in revised form 29 July 2009
Available online 31 August 2009

Keywords:
Boiling heat transfer
Dielectric liquid
Impinging jet
Single-phase convection

ABSTRACT

We have investigated the single-phase and boiling heat transfer of dielectric liquid under the Reynolds numbers (2000, 3000 and 5000) and under nozzle-plate spacing (H/W; 0.5, 1.0 and 4.0) in a submerged impinging jet system. The boiling incipience increases in proportion to the Reynolds number and in inverse proportion to the nozzle-to-surface spacing. The critical heat flux at $H/W = 1.0$ is lower than those of outer spacings, such as $H/W = 0.5$ and 4.0, due to the characteristics of the jet impingement heat transfer distribution. We suggest a correlation equation of nozzle-plate spacing (H/W) having the lowest CHF for various jet velocities.

1. Introduction

Jet impingement in forced convection heat transfer has become well established as a high-performance technique for the cooling, heating, or drying of surfaces. Jet impingement is applied in diverse industries, such as the cooling of gas turbine blades, annealing of steel plants, and the drying of paper and textiles. Electronic cooling has been actively researched as a superior solution to jet impingement, affording such benefits as increased power dissipation in chips with ever higher component-densities. Spray or jet impingement cooling with phase change offers excellent cooling performance in high heat flux devices. Boiling heat transfer characteristics are one of the most important research subjects pertaining to dielectric liquids. Confined jets under low spacings and low flow rates are also inevitable in many applications due to spatial claims or installation limitations.

The boiling is initiated on the surface when the wall superheat becomes sufficient to cause vapor nucleation on the surface. That is, onset of nucleate boiling (ONB) is generated. In the nucleate boiling regime, the bubbles transport the latent heat of the phase change and also increase the convective heat transfer by agitating the liquid near the heating surface. The vapor at some high heat flux forms an insulating blanket covering the heating surface and thereby raises the surface temperature. The boiling has sometimes been limited by a condition called critical heat flux (CHF). The most critical problem is the boiling limitation. It can be directly related to the burnout of a heated surface due to the suddenly inefficient heat transfer. Therefore, the many practical applications should be used in the boiling regime of single-phase convection to nucleate boiling. Numerous researchers [1–7] have studied single-phase to boiling heat transfers and critical heat flux of liquid jets including gases. They found that the enhancement of CHF is generally obtained through swirl flow, extension of the heated area, increasing the roughness of heated surface, and by increasing the turbulent level.

In addition, in order to optimize the performance in a system, the various gases and liquids have been applied to the system. Dielectric liquids, such as the fluorocarbons made by 3M Inc., are directly applied to electronic devices. They are nontoxic, chemically inert to packaging materials, and possess high dielectric strengths. They also have relatively low critical pressures, thermal conductivity and specific heats, and are largely air soluble. The extreme wettability of these fluids causes boiling hysteresis after superheat excursion results from large boiling incipience. There exists a need to diminish the temperature drop at the boiling incipience and to elevate the critical heat flux, which is the upper limit of nucleate boiling heat transfer. However, there has been insufficient effort to limit local boiling heat transfer by jet impingement with dielectric liquid.

Wadsworth and Mudawar [8–10] conducted experiments to investigate single-phase heat transfer from a smooth simulated chip to a two-dimensional jet of dielectric Fluorinert FC-72. They examined the effect of jet width, confinement channel height, and impingement velocity using this liquid. They also used a simulated chip constructed from an oxygen-free copper block soldered to a commercially available thick film resistor. They reported that the single-phase heat transfer was augmented considerably by

* Corresponding author. Tel.: +82 2 2123 2828; fax: +82 2 312 2159.
E-mail address: hhcho@yonsei.ac.kr (H.H. Cho).

0017-9310/$ - see front matter © 2009 Elsevier Ltd. All rights reserved.
doi:10.1016/j.ijheatmasstransfer.2009.08.002

Nomenclature

G	mass velocity (kg/m^2 s)	V_n	averaged velocity of a jet
H	nozzle-to-surface distance	W	nozzle width
l_h	heated length	x	streamwise distance from stagnation line
ONB	onset of nucleate boiling	y	vertical distance from heated surface
q''	heat flux	z	lateral distance from the center (origin)
Re	Reynolds number	ΔT_{sub}	degree of subcooling
T_{in}	average coolant temperature at nozzle inlet		
T_w	local wall temperature on target surface		

increasing velocity and delaying boiling incipience to a point of higher heat flux and surface temperature. They found that the nucleate boiling data appeared to fall on a single line, despite the increase in velocity. Both the surface heat flux and the surface temperature corresponding to incipience increased with increment of subcooling. However, the paper did not discuss the temperature overshoot at the point of boiling incipience; moreover, the thick copper block heater, which was used in this study, was not shown to vary local boiling heat transfer associated with jet impingement.

Thus, Ma and Bergles [11] investigated the characteristics of nucleate boiling with a circular jet impingement. They used R113 as a working fluid and jet tubes with inside diameters of 1.07 or 1.81 mm. They used the heated surface, which was made of a strip of 10-μm-thick constantan foil with heated sections of 5×5 or 3×3 mm^2. As a result, they found that the boiling curve at the stagnation point with high jet velocity was displaced to the right of the curve at the parallel flow region. Zhou and Ma [12] investigated a natural convection to burnout based heat transfer with an R113 impinging jet. They showed that the high heat flux regime of the nucleate boiling curve was independent of the jet parameters and was shifted to the left with elevated fluid subcooling. Thus, pool and impingement boiling may be described by the same equation as subcooling. Zhou et al. [13] also investigated boiling hysteresis with highly wetting liquids, R113 and L12378 (PF-5052). Those experiments were conducted with displaced nozzle locations so that the whole heat transfer regime could be considered repeatable in a steady state condition. They suggested that the incipience of boiling superheating decreased with fluid subcooling, and that superheat excursion increased with nozzle diameter, radial distance from the stagnation point, jet exit velocity and fluid subcooling. However, the repeatability of boiling incipience was determined to be poor at each location due to using the displaced nozzle. As such, the local heat transfer or wall temperature in the nucleate boiling regime should be measured simultaneously in lateral directions.

Nakayama et al. [14] investigated boiling heat transfer from forced convection in a planar impinging flow using fluorocarbon FX3250 (PF5050). They simulated a chip array with five (4 mm wide) strip heaters made of constantan foil with a thickness of 10 μm. They observed the transition from single-phase heat transfer to partial boiling accompanied by a temperature overshoot from the center strip. Their observed transitions and CHF were dependent on the jet velocity and subcooling. In their experiments, the local heat transfer was only measured at a stagnation point because just one thermocouple was installed on the center strip with a width of 4 mm ($x/W = 2$). They did not investigate measurements recorded in the lateral direction in the stagnation region, $x/W \sim 2$, in which the heat transfer rate varied intensely. Inoue et al. [15] investigated the CHFs of pure water in the confined flow of two-dimensional jet on flat and concave surfaces in the various flow conditions and measured the CHF at the different downstream positions. They found local CHF profile of the confined jet flow cooling system on the surface curvature heater. To evaluate the transition from a local jet impingement heat transfer to a boiling heat transfer for a free-surface, a planar jet of water with a thin-plate heater (thickness = 0.297–0.635 mm) was also employed by Wolf et al. [16–18] and Vader et al. [19].

Planar jet impingement provides a larger impingement zone than a circular jet while ensuring uniform coolant rejection following impingement. Under jet impingement, heat transfer variation is intense in the streamwise direction in single-phase convection. It is worth noting that heat transfer associated with jet impingement should be investigated not only for single-phase convection, but also for boiling heat transfer through local measurements. First, local single-phase convection and nucleate boiling heat transfer of dielectric liquid jet impingement are investigated with a thin-plate heater. Next, the present study focused on two parameters such as fluid flow rate and nozzle-to-surface spacing in conditions of confined wall and submerged liquid level. Finally, we found the nozzle spacings with the lowest CHF for the various mass velocities and then made a correlation for avoiding the bad nozzle spacings.

2. Experimental methods

2.1. Experimental apparatus

Fig. 1 presents the schematic view of experimental apparatus. The test loop comprises the main and secondary reservoirs, which control system temperature and pressure, condense the vaporized coolant, and degas the coolant; a magnetic pump; a mass flowmeter; the heat exchanger, which is connected to a constant temperature bath to regulate the jet temperature delicately; and a test section equipped with a regulated DC power supply and a data acquisition system. In the present study, the dielectric coolant or solvent for the electronic devices selected PF5060 manufactured by 3M.

Fig. 2 shows the schematic view of test section. The test section comprises the front, body, and rear panels. The front panel is made of a transparent polycarbonate plate for visualization of the nucleate boiling procedure. The rear panel is made of acryl. Inlet and outlet pressures are measured at pressure taps, and the jet and outlet temperatures are measured at the inlet connection, outlet and bypass using thermocouples. From these measured pressures and temperatures, the flowrate of the dielectric coolant is regulated by the inverter of the magnetic pump, the by-pass valve and the flow control valve upstream of the test section. The flow temperature is controlled by the thermocouple embedded in the inlet and the heat exchanger connected to a constant temperature bath. In addition, the pipes connecting each part are insulated by the materials with low thermal conductivity. The body, which is made of polycarbonate panels, forms the flow lines from a planar nozzle with inlet and outlet plenum. The nozzle dimensions are 2.0 mm (W) $\times$ 10.0 mm ($5W$). The width of the flow path ($5W$) is long enough to regard two-dimensions flow. To develop a fully velocity

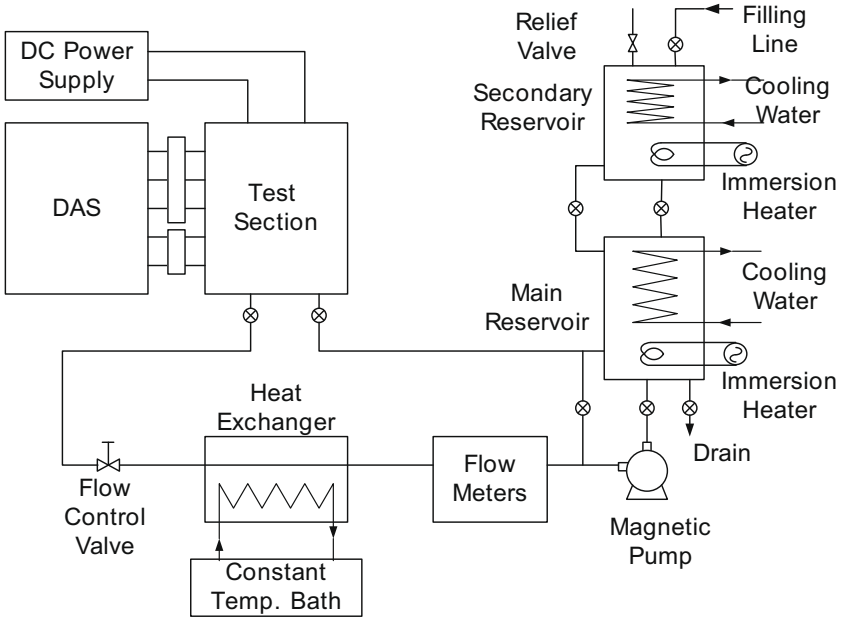

Fig. 1. Schematic view of experimental apparatus.

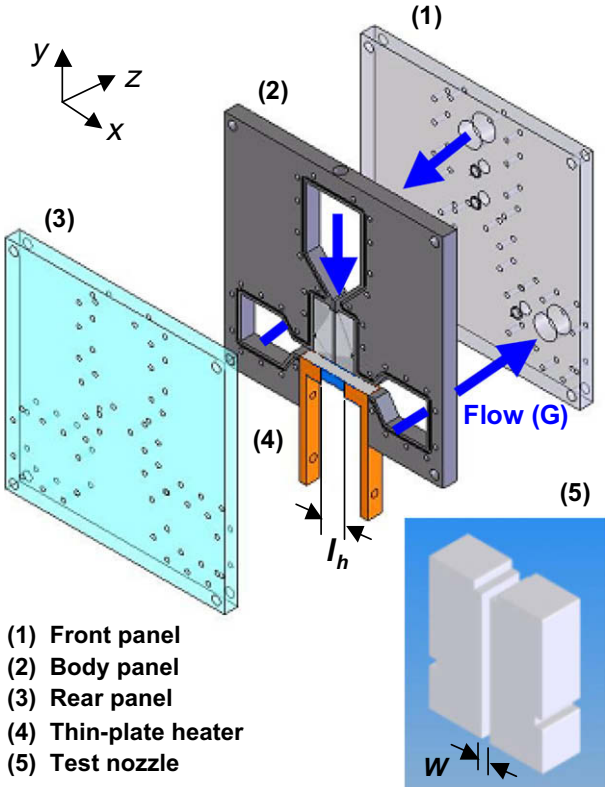

Fig. 2. Schematic view of test section.

profile at the nozzle exit, the length of straight flow is made to be 20 times of its width (W).

Fig. 3 presents the heater assembly used to measure the local wall temperature. The DC power supply is connected to the bus bar (copper block) soldered to the heater at the center of the impingement surface. The thin-plate heater made of INCONEL alloy 600 is applied to measure nucleate boiling heat transfer near the stagnation region. The INCONEL heater is 467 μm thick, 8 mm wide and 50 mm long, but only the central 10 mm is heated. To measure the wall temperatures, the seven thermocouples of K-type of 127 μm-diameter wires are welded to the backside of the heater 1 mm pitch along the center line. Current of the heater is measured using a shunt inserted in the middle of the power leads. To measure the voltage decrement associated with heating, the voltage taps are installed at location separated by 8 mm. From the voltage difference, the change of resistance of the heater is determined. The voltage signals of the thermocouples, the pressure transducers and the flowmeters are collected by a data logger (34970A, Agilent Technologies) and data sets are forwarded to a PC. The dry side is maintained by coating the test section with silicon rubber as a sealant, and heat loss from the test section is minimized with filling glass wool insulation. The origin of the coordinate system is in the middle point of the heater surface in Fig. 3(b). Its location is the same to that of the center thermocouple in the thermocouples embedded in the heater. The x, y, and z coordinates indicate streamwise distance from stagnation line to the exit, vertical distance from heated surface to the nozzle, and lateral distance from the origin to the front panel, respectively. The detailed explanation of the experimental apparatus is described in the previous studies [6,7].

2.2. Experimental procedure

The experiments are conducted according to rigorous procedures to ensure repeatability. To make the test surface uniform, it is polished with sand paper #2000 and cleaned with isopropyl alcohol. After the test section is installed, it is degassed by heating the immersion heater in the main reservoir. Vapors released during degassing are condensed in a secondary reservoir, and the drain valve is closed to the main reservoir. After degassing, the bulk fluid in the main reservoir is brought to a subcooled condition. The whole system is run for at least 1 h without operating the heater to age the heated surface.

Three nozzle-to-surface spacings of planar jets with dielectric liquid, PF5060, are examined for H/W = 0.5, 1.0 and 4.0 with the degree of subcooling, ΔT_{sub} = 25 °C and the corresponding bulk coolant temperature at nozzle inlet (T_{in}) of approximately 31 °C. Velocity effects are also considered for the average velocity of jet

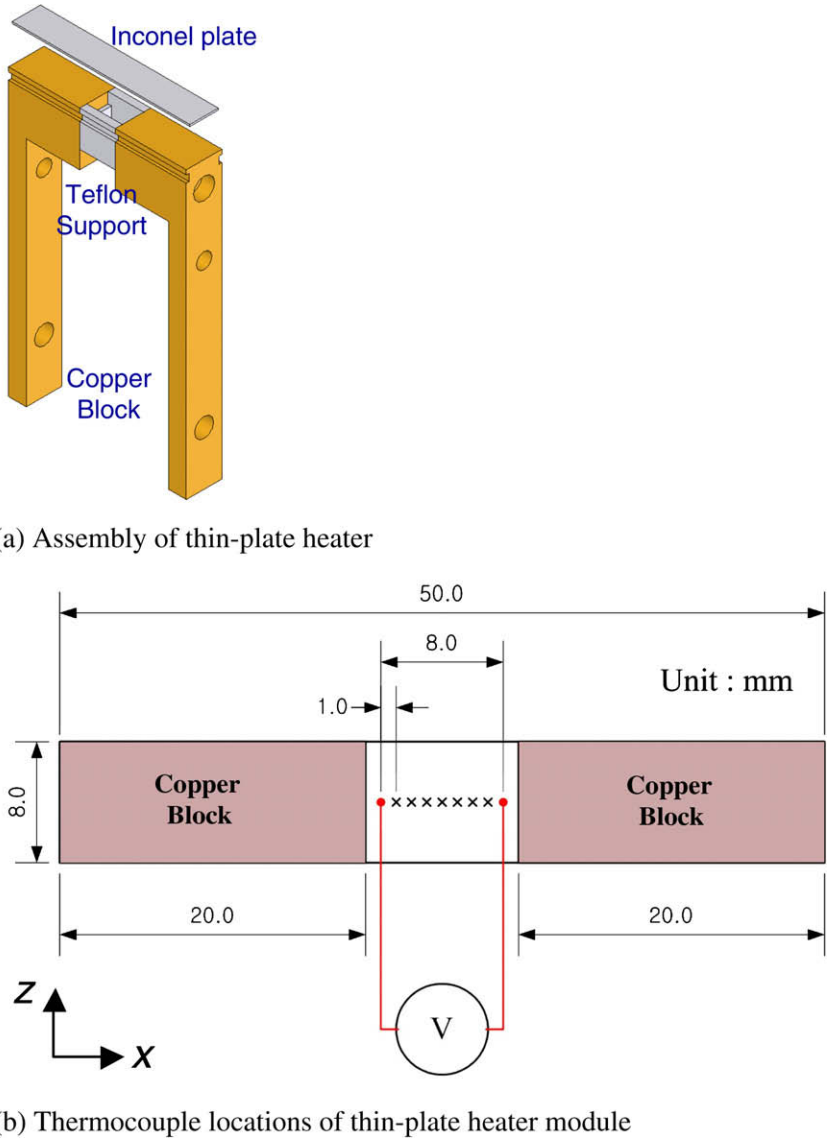

Fig. 3. Schematic view of thin-plate heater assembly.

(V_n) of 0.20, 0.31 and 0.52 m/s, from which the Reynolds numbers based on the hydraulic diameter of nozzle are calculated to be 2000, 3000 and 5000, respectively. Since the largest H/W is 4.0, the average jet velocity variation in the pre-impingement region caused by gravitational acceleration was negligible. Assuming one-dimensional conduction in the thin heater (y direction), local temperatures measured from the thermocouples welded to the backside of the heater are converted to the wall temperatures of the wetted surface. Wu et al. [6] and Shin et al. [7] calculated that, for a system of similar thickness and thermal properties, two-dimensional finite control volume approach obtained a temperature difference of less than 0.23 °C as compared with the one-dimensional conduction case.

To obtain each local wall temperature, we averaged 70–150 data measured at each location. The uncertainty analysis method developed by Kline and McClintock [20] revealed an overall uncertainty of ±2.8 °C for wall temperature; 2.64% for heat flux with 0.5% heat loss by radiation and conduction; 10.3% for the convection coefficient; 1.73% for the average velocity at the nozzle exit; 2.08% for the Reynolds number.

3. Results and discussion

Fig. 4 presents the wall temperature behaviors at the stagnation region on a submerged planar jet impingement for $Re \approx 3000$ and $H/W = 0.5$, 1.0 and 4.0. For all the nozzle spacings, the wall temperature (T_w) increases at a heat flux in the single-phase convection with increment of the distance from the jet center line (x/W); furthermore, the boiling incipience is initiated in the farthest downstream region. The reason is that heat transfer decreases (wall temperature increases) as the location goes away from the center.

At the longest nozzle-plate spacing ($H/W = 4.0$), the boiling incipience in downstream region ($x/W = 1.5$) is initiated at the heat flux of $q'' = 10.0\ \mathrm{W/cm^2}$ and the wall temperature of $T_w = 80.1$ °C; however, the inception at the stagnation point ($x/W = 0.0$) is initiated at higher heat flux of $q'' = 14.0\ \mathrm{W/cm^2}$ and lower temperature of $T_w = 78.5$ °C. The temperature drop in downstream region ($x/W = 1.5$) is observed at the heat flux of $q'' = 14.8\ \mathrm{W/cm^2}$ and the wall temperature of $T_w = 78.2$ °C. The downstream temperature drop is processed in the wide range of heat flux, while the temperature drop at boiling incipience is completed at its end and across

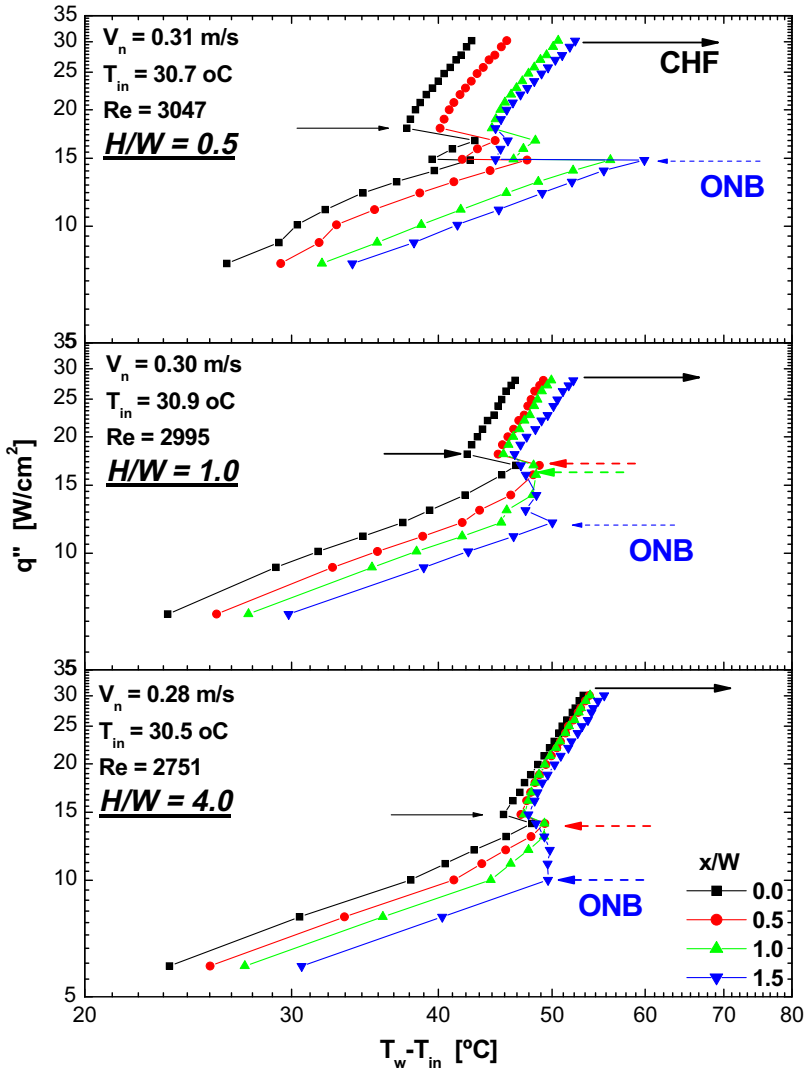

Fig. 4. Boiling curves at the stagnation region on a planar jet at $Re \approx 3000$.

the whole heated length including the stagnation point, $x/W = 0.0$. The wall temperature increases linearly in log scale with increasing heat flux in the fully developed boiling region. The ratio of heat flux to the wall temperature is much larger than that of the single-phase convection region. The wall temperatures at the fully-developed boiling regime are nearly uniform across the heated surface. The wall temperature at the fully developed boiling regime is little affected by the streamwise distance (x) from the impinging jet at $Re = 3000$ and $H/W = 4.0$.

In case of $H/W = 1.0$, the trends of single-phase convection and boiling incipience are similar to the results of $H/W = 4.0$. At the fully developed boiling region, however, the wall temperature is increased with increasing distance from the center line. In this region, the spatial variations of heat transfer along the distance from the stagnation point of jet impingement occur even in the fully developed boiling regime. The effects of jet impingement in the fully developed boiling regime are also presented in the lowest nozzle-to-surface spacing ($H/W = 0.5$). The difference of wall temperature in the stagnation region is distinctly presented in the fully developed boiling regime. For example, the average difference of wall temperature between the stagnation point ($x/W = 0.0$) and the downstream point ($x/W = 1.5$) is 2.1, 5.6 and 9.6 °C for $H/W = 4.0$, 1.0 and 0.5, respectively. It is because the proportion of vapor bubbles in the downstream region increases under the fully developed boiling condition with the decrement of the nozzle-to-surface spacing as shown in Fig. 5 (which is the photographs compared $H/W = 4.0$ with $H/W = 1.0$ at $Re \approx 3000$). Although the width of the flow path (5 W) is long enough to regard two-dimensions flow, the wall temperatures are measured in the middle points of flow path to reduce the effects of side walls.

At the nozzle-to-surface spacing of $H/W = 4.0$, the fully developed boiling regime is initiated at the heat flux of $q'' = 14.8$ W/cm^2. As shown in Fig. 5(a), the vapor bubble on the heated surface at the heat flux of $q'' = 16.0$ W/cm^2 is distributed across the whole surface, including the stagnation point. However, at a spacing of $H/W = 1.0$, as shown in Fig. 5(b), the bubble at the stagnation point appears intermittently, where the bubble is absent partially at the stagnation zone despite a fully developed boiling regime for the high heat flux of $q'' = 22.0$ W/cm^2. It is noted that the critical heat flux is 29.1 W/cm^2 in this case. The vapor bubble near the stagnation point is eliminated quickly due to the liquid jet impingement, however the confined channel is occupied fully by bubbles at the downstream region.

Fig. 6 compares the boiling curves at the nozzle-to-surface spacing of $H/W = 4.0$ for the three different Reynolds numbers. The temperature drop is initiated farther downstream and completed with the temperature drop at the stagnation point. The heat flux and the wall temperature at the boiling incipience are increased largely

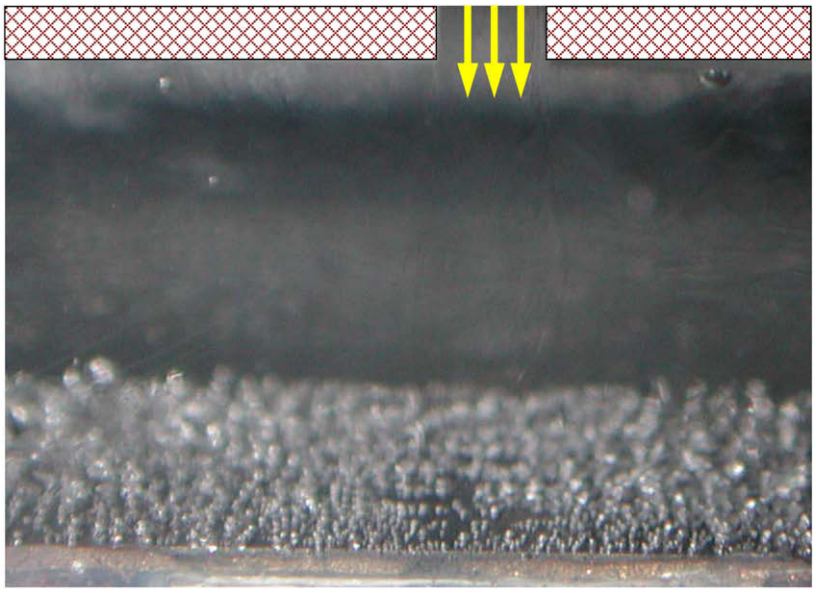

(a) Re=2,847, H/W=4.0, q"=16.0 W/cm^2

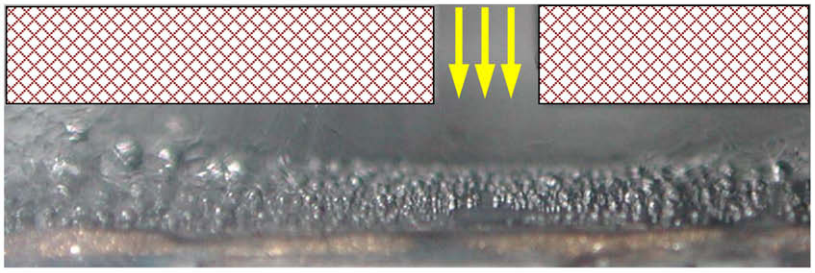

(b) Re=2,995, H/W=1.0, q"=22.0 W/cm^2

Fig. 5. Photographs in the fully developed boiling regime at $Re \approx 3000$ for $H/W = 1.0$ and 4.0.

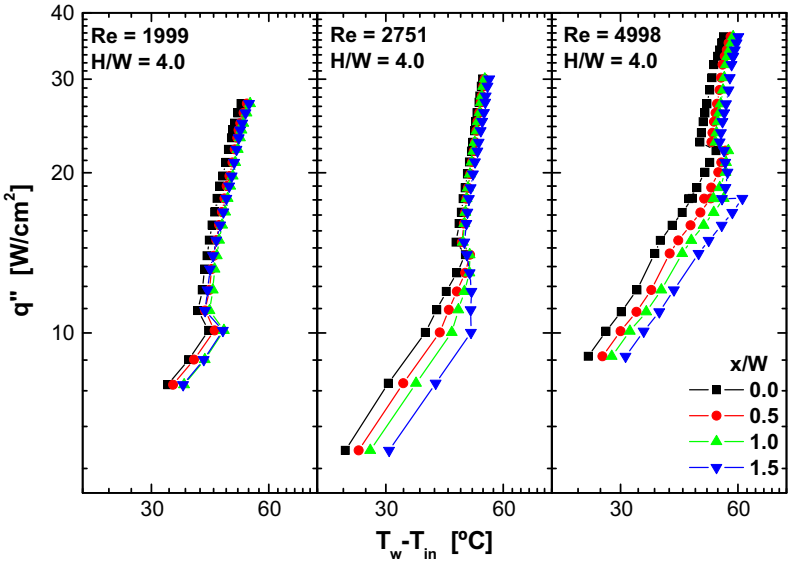

Fig. 6. Effect of impinging jet Reynolds number on boiling curves for $H/W = 4.0$.

with increasing the impinging jet velocity, while the downstream temperature drop proceeds more gradually. The critical heat flux increases with increasing the impinging jet Reynolds number. It is noted that the increment (9.3 W/cm^2) of critical heat flux is not big as that (11.9 W/cm^2) of heat flux at the boiling incipience (or the starting point of full boiling) with increasing the impinging jet Reynolds number. The reason might be that the generated bubbles have a strong buoyancy force against to the impingement jet

in the fully developed boiling regime. Thus, the impinging liquid jet cannot reach properly near the heater surface. In the fully developed boiling regime, temperature differences between the stagnation point ($x/W = 0.0$) and the downstream point ($x/W = 1.5$) increase slightly with increasing the Reynolds number. At the lowest Reynolds number of about 2000, the wall temperature at the stagnation point of $x/W = 0.0$ is slightly lower than those of $x/W = 0.5$–1.5. However, at the highest Re of about 5000, the wall temperature difference becomes higher than that of $Re = 2000$. The reason is that the heat transfer and momentum differences of the impingement jet in the streamwise direction (x/W) exit even in the fully developed boiling regime.

The spacing effects at $x/W = 0.0$ and 1.5 are compared for $Re = 3000$ in Fig. 7. The boiling incipience increases as the nozzle-to-surface spacing decreases. That is, the temperature drop with boiling incipience at the spacing of $H/W = 0.5$ is the largest at the stagnation point ($x/W = 0.0$) as well as the downstream point ($x/W = 1.5$). The reason is that the jet impingement influences the total heat transfer rate even in the fully developed boiling regime as the nozzle-to-surface spacing decreases. The temperature difference in the nozzle spacing between $H/W = 0.5$ and $H/W = 4.0$ is large at the stagnation point in the fully developed boiling regime; however, the difference is reduced at the downstream. It is because the vapor bubbles under the low nozzle spacing are eliminated quickly at the stagnation point due to the strong impingement jet momentum, while the bubble occupied area increases in the downstream region with the narrow spacing and reduced the jet momentum. Consequently, the jet impingement effects in the fully developed boiling regime increase at the central position as the jet velocity increases and/or the nozzle-to-surface spacing decreases.

Fig. 8 shows the averaged wall temperature for various Reynolds numbers and the nozzle-to-surface spacings. The wall temperature is averaged along the streamwise direction (2D jet).

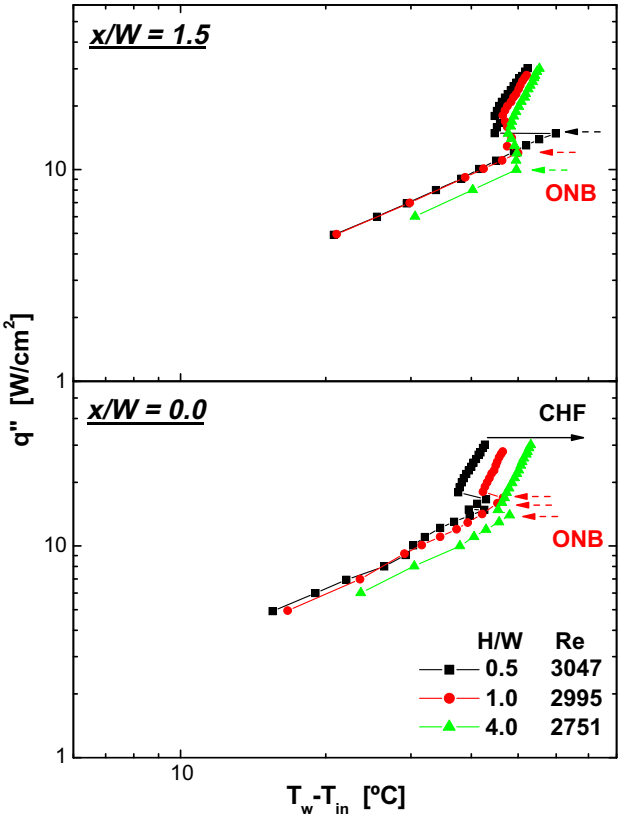

Fig. 7. Effect of nozzle-to-surface spacing on local boiling curves at $Re \approx 3000$.

Therefore, the line averaged wall temperature corresponds to the averaged value of the whole heated area. For the spacing of $H/W = 4.0$, the averaged wall temperature in the fully developed boiling regime is independent of the Reynolds number despite the big difference in the single-phase convection regime as presented in Fig. 8. Studying a copper block heater which obtains only average values, Wadsworth and Mudawar [9] mentioned that the single-phase heat transfer significantly increased with increasing velocity, and that the point of boiling incipience was delayed to a higher heat flux and a higher surface temperature with increasing velocity. Despite an increase in velocity, the nucleate boiling data seemed to fall on a single line. The averaged wall temperature results presented herein are in good agreement with those obtained by Wadsworth and Mudawar [9]. As the spacing decreases to $H/W = 1.0$, the wall temperature at the Reynolds number of 3000 and 5000 in the fully developed boiling regime is slightly lower than that at the lower Reynolds number of 2000; furthermore, at the small spacing of $H/W = 0.5$, the heat transfer performance increases with increasing the Reynolds number in the fully developed boiling regime. The temperature drop at the small spacing of $H/W = 0.5$ is also increased sharply with increment of the Reynolds number. The reason is that the central momentum of the impingement jet flow is strengthened as the nozzle spacing decreases and/or the jet velocity increases. It is noted that the jet velocity effect is little at the large spacing, but it is more strengthened with decrement of the spacing.

The critical heat flux data obtained in the experiments of heated length, $l_h = 10$ mm, are plotted for various nozzle-to-surface spacings in Fig. 9. A critical heat flux correlation induced from the experimental data is expressed to second-order function of impinging jet height-to-width and mass velocity as following equation:

$$q''_{CHF} = 17.47\log(G)^2 + 8.5831\log(10\times H/W)^2 + 11.7931 \times \log(G)\log(10\times H/W) - 83.7\log(G) - 50.251 \times \log(10\times H/W) + 138.1 \quad (1)$$

The critical heat flux increases as mass flow rate (jet velocity) increases, and that is consistent with a typical trend of CHF. In the present experiments, the critical heat flux at the spacing of $H/W = 1.0$ is lower than those of other spacings of $H/W = 0.5$ and 4.0. This trend is observed in tested whole mass flux conditions. Considerable heat transfer enhancement of jet impingements with the low spacing is resulted from significant increases of the turbulence intensity by acceleration of the impinged flow and velocity discrepancy between the accumulated flow and the impinged flow. The mechanism results in high heat transfer in wide wall jet region. It is called secondary peak, which is well-known as one of the heat transfer characteristics induced by impinging jet with low spacing [6,7,21]. However, as the nozzle-plate spacing increases, the heat transfer rate of the impinging jet is reduced, and the high heat transfer region becomes narrow. Thus, at a long nozzle-plate spacing, the heat transfer rate is related to the mass flow rate. Because the CHF is also enhanced by heat transfer rate, the high CHF at $H/W = 0.5$ is observed by the high heat transfer rate of impinging jet flow, while the low CHF at $H/W = 1.0$ appears due to the reduced flow velocity near the surface and resulting the low heat transfer rate. However, the CHF increases at the larger nozzle-plate spacing of $H/W = 4$, especially at the high mass flow rate of $G = 842$ kg/m^2 s ($Re = 5000$). The high flow velocity generates the high heat transfer, and the large spacing helps to remove the generated bubbles from the boiling surface for a confined channel, so that CHF increases at the high mass flow rate and the large nozzle-plate spacing with the delayed starting point of film boiling. This effect is enhanced largely with increasing mass flow rate. Therefore, there is a nozzle-to-surface spacing having a minimum CHF

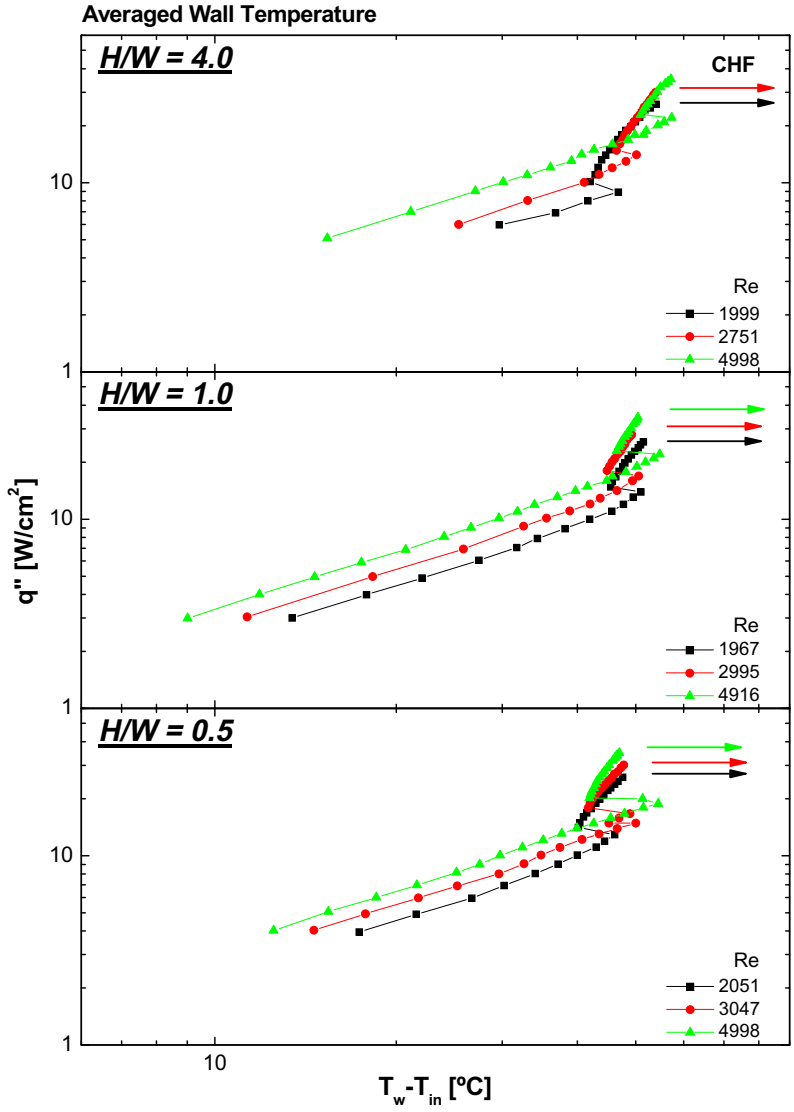

Fig. 8. Averaged wall temperature for various jet Reynolds numbers and nozzle-to-surface spacings.

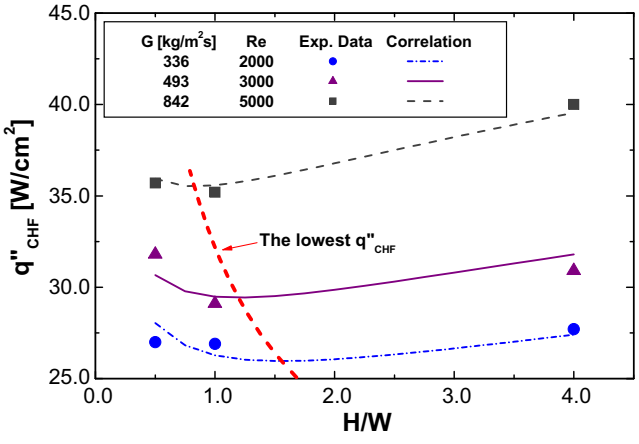

Fig. 9. Effect of nozzle-to-surface spacing and jet velocity on critical heat flux.

for a certain mass flow rate (or jet velocity). The reason is that the boiling heat transfer at the stagnation region increases with decreasing the spacing due to high jet impingement effect, and reversely the boiling heat transfer on the downstream region increases with increasing the spacing due to the enough spacing of removing bubbles. In an actual design, the geometry of impinging jet keeps away from *H/W* with the lowest critical heat flux because the low critical heat flux causes the low system performance. Therefore, the optimum nozzle-plate spacing should be selected for enhancing the performance. Thus, we have found the impinging jet nozzle-to-surface spacing *(H/W)* with the lowest CHF at each mass velocity (*G*). It is expressed as following equation:

$$[H/W]_{lowestCHF} = 1.4016\log(G)^2 - 9.4548\log(G) + 16.493 \qquad (2)$$

4. Conclusions

This study examines the effects of single-phase convection and nucleate boiling heat transfer of dielectric liquid in a submerged and confined impinging jet mode. Heat transfer behaviors on a planar liquid jet impingement are studied under the Reynolds numbers of 2000, 3000 and 5000 and under the spacing of *H/W* = 0.5, 1.0 and 4.0.

Downstream temperature drop is processed across a wide range of heat fluxes; the temperature drop at the boiling incipience is

completed such that boiling incipience occurs over the whole heated length, including the stagnation point. At the fully developed boiling regime, the wall temperature is increased with increasing distance from the center line, and the spatial variations of heat transfer along the streamwise direction of jet impingement appear in this test because the difference of heat transfer exists in the fully developed boiling regime. The wall temperature difference along the nozzle-to-surface spacing at the stagnation point is distinctly presented in the fully developed boiling regime. As the nozzle-to-surface spacing decreases, the vapor bubbles near the stagnation point are eliminated by the liquid jet with the strong momentum of impinging jet at the center. That is, the effect of the jet on the fully developed boiling regime is increased with increasing jet velocity and is increased with decreasing nozzle-to-surface spacing.

The critical heat flux (CHF) at the spacing of $H/W = 1.0$ is lower than those of other spacings of $H/W = 0.5$ and 4.0 under a constant mass flux (or constant jet velocity) conditions. As the nozzle-plate spacing increases, the generated bubbles are removed easily with the large spacing for a confined channel, especially for the large mass flow rate, while the heat transfer rate of the impinging jet is reduced at the stagnation region. Thus, at a long nozzle-plate spacing, the heat transfer rate increases on the downstream region. Otherwise, it is reverse for decreasing the spacing. Therefore, there is a nozzle-plate spacing having a minimum overall boiling heat transfer for a certain mass flow rate. In design of an actual cooling system, if the geometries and the operating conditions are similar to the present confined submerged impingement jet system, a designer must avoid to select a certain nozzle-plate spacing, such as approximately $H/W = 1$.

References

[1] H. Martin, Heat and mass transfer in between impinging gas jets and solid surfaces, Adv. Heat Transfer 13 (1977) 1–60.

[2] R. Viskanta, Heat transfer to impinging isothermal gas and flame jets, Exp. Therm. Fluid Sci. 6 (1993) 111–134.

[3] D.H. Wolf, F.P. Incropera, R. Viskanta, Jet impingement boiling, Adv. Heat Transfer 23 (1993) 1–132.

[4] B.W. Webb, C.F. Ma, Single-phase liquid jet impingement heat transfer, Adv. Heat Transfer 26 (1995) 105–217.

[5] M. Arik, A. Bar-Cohen, Immersion cooling of high heat flux microelectonics with dielectric liquids, in: International Symposium on Advanced Packaging Materials, 1998, pp. 229–247.

[6] S.J. Wu, C.H. Shin, K.M. Kim, H.H. Cho, Single-phase convection and boiling heat transfer: confined single and array circular impinging jets, International Journal of Multiphase Flow 33 (12) (2007) 1271–1283.

[7] C.H. Shin, S.J. Wu, K.M. Kim, H.H. Cho, Effects of planar jet impingement on single-phase convection and boiling heat transfer characteristics, JP J. Heat Mass Transfer 2 (1) (2008) 55–71.

[8] D.C. Wadsworth, I. Mudawar, Cooling of a multi-chip electronic module by means of confined two-dimensional jets of liquid, ASME J. Heat Transfer 112 (1990) 891–898.

[9] D.C. Wadsworth, I. Mudawar, Experiment of single-phase heat transfer and critical heat flux from an ultra-high-flux simulated microelectronic heat sourced to a rectangular impinging jet of dielectric liquid, ASME J. Heat Transfer 114 (1992) 764–768.

[10] I. Mudawar, D.C. Wadsworth, Critical heat flux from a simulated chip to a confined rectangular impinging jet of dielectric liquid, Int. J. Heat Mass Transfer 34 (1991) 1465–1478.

[11] C.F. Ma, A.E. Bergles, Jet impingement nucleate boiling, Int. J. Heat Mass Transfer 29 (1986) 1095–1101.

[12] D.W. Zhou, C.F. Ma, Local jet impingement boiling heat transfer with R113, Heat Mass transfer 40 (2004) 539–549.

[13] D.W. Zhou, C.F. Ma, J. Yu, Boiling hysteresis of impinging circular submerged jets with highly wetting liquids, Int. J. Heat Fluid Flow 25 (2004) 81–90.

[14] W. Nakayama, M. Behnia, H. Mishima, Impinging jet boiling of a fluorinert liquid on foil heater array, ASME J. Electron. Packag. 122 (2000) 132–137.

[15] A. Inoue, A. Ui, Y. Yamazaki, S. Lee, Studies on cooling by two-dimensional confined jet flow of high heat flux surface in fusion reactor, Nucl. Eng. Des. 200 (2000) 317–329.

[16] D.H. Wolf, R. Viskanta, F.P. Incropera, Local convective heat transfer from a heated surface to a planar jet of water with a nonuniform velocity profile, ASME J. Heat Transfer 112 (1990) 899–905.

[17] D.H. Wolf, F.P. Incropera, R. Viskanta, Local jet impingement boiling heat transfer, Int. J. Heat Mass Transfer 39 (1996) 1395–1406.

[18] D.H. Wolf, Turbulent development in a free-surface jet and impingement boiling heat transfer, Ph.D. Thesis, Purdue University, West Lafayette, IN, USA, 1993.

[19] D.T. Vader, F.P. Incropera, R. Viskanta, A method for measuring steady local heat transfer to an impinging liquid jet, Exp. Therm. Fluid Sci. 4 (1991) 1–11.

[20] S.J. Kline, F.A. McClintock, Describing uncertainty in single-sample experiments, Mech. Eng. 75 (1953) 3–8.

[21] D. Lytle, B.W. Webb, Air jet impingement heat transfer at low nozzle-plate spacings, Int. J. Heat Mass Transfer 37 (12) (1994) 1687–1697.